Characterisation of microcrystalline diamonds deposited by HFCVD

Tao Zhang, Feng Qin* and Wanghuan Qian

Mechanical Institute of Technology,
Wuxi Institute of Technology,
Wuxi 214122, China
Email: zhangt@wxit.edu.cn
Email: qinf@wxit.edu.cn
Email: qianwh@wxit.edu.cn
*Corresponding author

Lijun Zhang

School of Engineering Science and Technology,
Shanghai Ocean University,
Shanghai 201316, China
Email: ljzhang@shou.edu.cn

Fanghong Sun

School of Mechanical Engineering,
Shanghai Jiao Tong University,
Shanghai 201316, China
Email: sunfanghong@sjtu.edu.cn

Abstract: The performances of CVD microcrystalline diamond powders by the seeding and self-nucleation method, including the particle size composition, crystal morphology, and diamond purity, are evaluated by the China industry standard of conventional diamond powders (JB/T 7990-2012). The detection results show over 80% particles grown on the seeds exhibit a cubo-octahedral with smooth surfaces and no obvious growth defects, while they can hardly meet the corresponding commercial requirements of particle size composition due to the existence of 10%–23% spontaneous particles (0.5~1.2 μm). For the powders deposited by self-nucleation method, the particle size composition agrees well with the model defined by the industry standard, and 70.5% crystals exhibit the cubo-octahedral or icosahedron morphology, as well as their surface quality are little worse than those grown on the seeds due to unwanted secondary nucleation. Besides, the two types of CVD powders have a high purity detected by micro-Raman spectroscopy.

Keywords: microcrystalline diamond particles; morphology; particle size; hot filament CVD.

Reference to this paper should be made as follows: Zhang, T., Qin, F., Qian, W., Zhang, L. and Sun, F. (2018) 'Characterisation of microcrystalline diamonds deposited by HFCVD', *Int. J. Abrasive Technology*, Vol. 8, No. 4, pp.292–309.

Biographical notes: Tao Zhang works from the Mechanical Engineering Department at the Wuxi Institute of Technology, China. She graduated with a PhD degree in the School of Mechanical Engineering from the Shanghai Jiao Tong University, China in 2014. She had worked at the Shanghai Ocean University, China from July 2014–July 2017. She has published more than ten articles on many international journals, including *Journal of Crystal Growth*, *Surface and Coatings Technology*, and *Diamond and Related Materials*. Her research interests are fabrication and application of CVD diamond, and the research on 'A new synthesis technology of free-standing boron-doping microcrystalline diamonds' has been supported by National Natural Science Foundation of China.

Feng Qin is an Associate Professor from the Mechanical Engineering Department at the Wuxi Institute of Technology, China. He graduated with a PhD degree in Mechanical Engineering from the University of Alabama, USA in 2012. His research interests include metal cutting tools, surface integrity, and material manufacturing.

Wanghuan Qian is an Associate Professor from the School of Mechanical Engineering at the Wuxi Institute of Technology, China. He received his PhD in Mechanical Engineering at the Nanjing University of Aeronautics and Astronautics, China in 2014. His primary research interests include metal matrix composites synthesised by electroforming or chemical vapour deposition and surface treatment.

Lijun Zhang is a Lecturer from the Mechanical Engineering Department at the Shanghai Ocean University, China. She graduated with a PhD in Mechanical Engineering from the University of Nebraska-Lincoln, USA in 2008. Her research interests focus on large-scale molecular dynamics exploration of the thermophysical properties of nanoscale and nanostructured materials and laser-assisted imaging and characterisation of surface material in nanoscale.

Fanghong Sun is a Professor from the School of Mechanical Engineering at the Shanghai Jiao Tong University, China. His research interests include super-hard materials, metal cutting tools, and material manufacturing.

1 Introduction

Microcrystalline diamond powders (< 38 μm) have outstanding properties, making them suitable candidate abrasives widely employed in optical and electronic materials and components, focused on ultra-high precision finish machining processes (May, 1995; Filatov et al., 2013). The most practically artificial diamonds are synthesised by high-temperature and high-pressure method (HTHP-method). Owing to the method with a critical manipulating synthetic parameter, it is impossible to grow the isolated crystals with ultra-fine grain sizes. Therefore, the overwhelming microcrystalline diamonds (< 38 μm) are purified and selected from impurities obtained from smashing the large-sized ones (Sung, 1999; Schwarz et al., 2004).

Chemical vapour deposition (CVD) diamonds have generated substantial interest in recent decades due to many outstanding advantages, such as extremely high hardness, the deposited diamond crystals with well-controlled morphology and size, and smooth surfaces, together with the low energy consumption. A lot of achievements have been

achieved in the field of deposition and characterisation of diamond films (Abreu et al., 2006; Konoplyuk et al., 2007; Sun et al., 2009; Sochr et al., 2014; Boussadi et al., 2017) and large single crystals (Linares and Doering, 1999; Yan et al., 2004; Schreck et al., 2002; Achard et al., 2011; Shu et al., 2018). On that basis, some scientists have focused on how to fabricate isolated microcrystalline diamonds and inhibit films growth by CVD method. Some of them have applied a seeding initiation method to deposit microcrystalline diamonds (Schwarz et al., 2004; Hirmke et al., 2006; Stacey et al., 2009), and others have employed self-nucleation one (Chung and Sung, 2001; Chakraborty and Sharma, 2011). Each approach has its own pros and cons, which has been discussed in detail in Zhang et al. (2015) and Iniesta et al. (2001). The particles grown with the seeding generally have a very well morphology but a wide range of size. The particles deposited directly by the self-nucleation have a very narrow distribution on the grain size while some growth defections such as secondary nucleation and lattice distortion. To date, it is still a challenge to mass produce the microcrystalline diamonds with complete crystal shapes via CVD. Besides, to our knowledge, it has been rarely reported on characterisation of CVD diamond powders.

In our previous works, we attempted the above two initiation methods to deposit microcrystalline diamonds via HFCVD (hot filament CVD) apparatus. Then we found that the two approaches contribute to the diamonds with different distributions of grain sizes (Zhang et al., 2015; Zhang et al., 2013a, 2013b; Zhang and Zou, 2017). In this work, we summarise the previous works and provide the detailed techniques for depositing the microcrystalline diamonds with regular crystal shapes. Subsequently, the freestanding diamond powders are gained by chemical etching to remove silicon wafers and then collect crystals with a high-speed centrifugation. Thereafter, the performances of CVD powders, including the particle size composition, crystal morphology, and diamond purity, are evaluated against the industry standard of conventional diamond powders (JB/T 7990-2012), using field emission scanning electron microscopy (FESEM), micro-Raman spectroscopy, and electron backscattered diffraction (EBSD) techniques.

2 Experiment details

2.1 Fabrication of CVD microcrystalline diamonds with the seeding method

The HFCVD facility of 100 mm^2 deposition area (as detailed in Zhang et al., 2013a; Zhang and Zou, 2017) is employed to perform the deposition of microcrystalline diamonds grown on seeds, with 3-inch silicon wafer polished as the substrates, commercial diamond powders used as the seeds. Other conditions such as hot filament distribution mode, seeding method, boron doping method are shown in Zhang et al. (2013a, 2013b). Detailed deposition process parameters are listed in Table 1. It is found from the previous works (Zhang et al., 2013a, 2013b) that to improve the deposition rate of isolated diamonds, a wide variety of seed grains and different redeposition methods are employed according to the deposited diamonds of different sizes, seen in Table 2. Averagely 2–13 μm particles could be produced via the above method. It is needed to point out that the commercial powders sizing over W15(M8/16) might not be suitable as the seeds for the growth of superior isolated diamonds mainly. This is attributed to the fact that too many unwanted nuclei are grown spontaneously on the substrate close to

regrown particles, leading to the poly-crystals or even films formation most likely (Zhang et al., 2013a, 2013b).

Table 1 The deposition parameters for CVD microcrystalline diamonds by the seeding method

Parameters	*Growth parameters*
Acetone/hydrogen volume ratio	1.3%–1.4%
[B]/[C]gas (ppm)	0–500
Reaction pressure (kPa)	4.5
Substrate temperature (°C)	800–900
Hot filament temperature (°C)	2,200 ± 200
Bias current intensity (A)	1
Deposition time (min)	90–240

Table 2 The deposition parameters of CVD microcrystalline diamonds with different sizes via the seeding method

Seeds type	*[B]/[C]gas (ppm)*	*Deposition time (min)*	*Average size of as redeposited diamond (μm)*
W1	0	60~90	2.5
W2.5	0/500	240/120	5.0
W5	500	120	8.7
W10	500	480	12.6

2.2 Fabrication of CVD microcrystalline diamonds with the self-nucleation method

The substrate surface should be polished 0.5–1 min by 0.5 μm diamond powders, and then be ultrasound washed 3–5 min in deionised water and acetone solution. The nucleation and growth parameters can be referred to Table 3, with certain deposition time less than 120 min. Note that, overlong deposition time could result in the formation of too many poly-crystals or secondary nucleations on the crystal surfaces (Zhang et al., 2015). To improve the crystal growth rate appropriately, 500 ppm trimethyl borate is introduced into the reaction gas source. The method introduced here may gain diamonds sizing averagely 0.3–2 μm.

Table 3 The deposition parameters for CVD microcrystalline diamonds by the self-nucleation method

Deposition parameters	*Nucleation stage*	*Growth stage*
acetone/hydrogen volume ratio	1.5%	2.0%
[B]/[C]gas (ppm)	500	500
Reaction gas pressure (Kpa)	3	3
Bias current intensity (A)	4.0	4.0
Substrate temperature (°C)	700	950
Hot filament temperature (°C)	2,000 ± 200	2,200 ± 200
Deposition time (min)	40	~80

2.3 Collecting and purifying technique of CVD diamond powders

To collect the CVD microcrystalline powders, i.e., acquire the freestanding isolated particles, as-deposited species are required to be post-processed as the following process.

A Removing substrate: Normally, the silicon is inert to nitric acid, sulphuric acid, hydrofluoric acid, and hydrochloric acid whether at a concentrated condition or not while could interact with a mixture of nitric acid and hydrofluoric acid. Accordingly, the mixture of the two former acids in volume ratio of 1:1 is able to dissolve silicon substrate. The reaction is written as follows.

$$Si + 4HNO_3 \rightarrow SiO_2 + 2H_2O + 4NO_2 \quad (1)$$

$$SiO_2 + 6HF \rightarrow H_2SiF_6 + 2H_2O \quad (2)$$

HNO_3 in equation (1) generates a insoluble layer of silicon dioxide, which continues to react with the hydrofluoric acid to produce fluosilicate (complex compound, soluble in water), allowing the silicon surface to continue reacting and thereby producing (H_2SiF_6), therein consuming the silicon substrate.

B Removing the mixture of acid solution: A high speed centrifugal machine (TG1650-WS) is employed to perform particle sediment separation tests with 1,000 rpm speed setting and 5 mins long. After the separation process, the top layer of the mixed acid solution is drained slowly, then injection of distilled water to the remaining in particles suspension is carried out, meanwhile ultrasound vibration is utilised to do cleaning operation. The centrifugal-cleaning process is repeated 7–8 times to gain the neutral particles suspension.

C Particle distillation process: The diamond powders could be produced via the following dust-free operations, putting the particles suspension into a distillation flask and heating to remove the water solution.

3 Evaluation details

The diamond powders are generally examined on their particle size composition, crystal morphology, and diamond purity. In this work, the quality test of CVD diamond powders is taken as follows. Five hundred single crystal particles are chosen randomly in each specimen then their shapes and sizes are observed by FESEM and statistically recorded. Secondly, three crystals are picked up randomly in each specimen, and then evaluated on the diamond purity and the crystal integrity via micro-Raman spectrum and EBSD.

The particle size composition and crystal morphology of CVD diamond powders are evaluated against an industry standard of conventional diamond powders (JB/T 7990-2012, detailed in Table 4. Additionally, the commercial diamond powders are classified by the quality indexes of crystal morphology, shown in Table 5, where the irregular crystals include strips, sheets, needle shapes, and other strange shapes. It is noted that the crystal morphologies of type 1 powders are slightly better than that defined by US industry standard of ANSI B74.20-1981, and type 2 ones have superior performances and are considered as ‘high quality crystal shape diamond powders’. The

diamond purity can be calculated and evaluated according to equation (3) shown as follows.

$$q = \frac{75 \cdot I_d}{75 \cdot I_d + \sum_{nd} I_{nd}} \cdot 100\% \tag{3}$$

where I_d is the intensity of Raman diamond peak, and I_{nd} shows the sum intensity of sp^2 phases peaks (Silva et al., 1996). A Raman signal efficiency factor ratio of 75 between the sp^2 and the diamond phases is used (Wada and Solin, 1981).

Table 4 The quality index of grain size and size distribution for the commercial diamond powders produced by crushing the large-sized HPHT diamonds

Type	*Nominal size*	D_5	D_{50}	D_{95}	*Largest size*
	D/μm	*μm*	*μm*	*μm*	*μm*
M0/0.5 (W0.5)	~0.5	-	0.25 ± 0.05	0.5	1.5
M0/1 (W1)	~1	-	0.5 ± 0.10	1.0	3.0
M1/2 (W2.5)	1~2	1.0	1.5 ± 0.22	2.0	6.0
M2/4 (W4)	2~4	2.0	3.0 ± 0.30	4.0	9.0
M3/6 (W5)	3~6	3.0	4.5 ± 0.45	6.0	12.0
M4/8 (W7)	4~8	4.0	6.0 ± 0.6	8.0	15.0
M6/12 (W10)	6~12	6.0	9.0 ± 0.9	12.0	20.0
M8/16 (W15)	8~16	8.0	12.0 ± 1.2	16.0	24.0
M10/20 (W20)	10~20	10.0	15.0 ± 1.5	20.0	26.0

Notes: D_5 – fine end granularity index, representing the particle size on the cumulative distribution curve of the particle sizes at a cumulative frequency of 5%.
D_{50} – median diameter index, representing the particle size on the curve at a cumulative frequency of 50%.
D_{95} – coarse end granularity index, representing the particle size on the curve at a cumulative frequency of 95%.

Source: According to an China industry standard, JB/T 7990-2012, for diamond powders

Table 5 The quality index of morphology for the commercial diamond powders produced by crushing the large-sized HPHT diamonds

Type	*Irregular shapes / %*	*Narrow strips / %*
1	< 15	< 3
2	< 7	0

4 Results and discussions

4.1 Quality evaluation of CVD diamond powders grown on seeds

The seeds sizing less than W5 are suitable for an intrinsic process regrowth. Firstly, the evaluation of the fixed W1(M0/1) seed is instanced here. Secondly, the seeds of W5–W15(M3/6–M8/16) are performed regrowth process via 500 ppm boron-doping technique. In the following, the performances of W5(M3/6) seeds are evaluated.

M0/1 commercial diamond powders could scatter uniformly on the silicon-based substrate surface via the self-created seeding method. The surface flaw of seeds is totally covered by the newly grown diamond crystal surface after 90 mins intrinsic deposition, shown in Figure 1(a). One hundred thirty million particles may be collected on the 100 cm^2 substrate through one deposition. 500 particles among them are chosen randomly to perform size checking and morphology statistics, shown in Figure 1 and Table 6. The size falls into 0.5–4.5 μm, among which 75% sizing at 2–4 μm, closing to the size of M2/4 model in the powder standards. The particles reach coarse end granularity index (D_{95}) corresponding to the powder model and the requirement of the max particle size while not satisfy the fine end granularity index (D_5) and median diameter index (D_{50}) due to the existence of 9% spontaneous particles (0.5~1.0 μm) in the powders. Morphological statistics show that 85.5% single crystal powders display the cubic morphology framed by octahedron with smooth surface and negligible growth flaw. It demonstrates that under the certain deposition conditions, the growth rate of one crystal face for each particle is similar, then leading to similar crystal morphology of most particles [$1.5 < \alpha < 3$, $\alpha = (3)^{1/2}V_{100} / V_{111}$ (Gicquel et al., 2001)]. Such crystal shape items are listed as follows: grain plumpness b greater than 50%, grain prismatic face angle γ around 125°, Φ (300°–330°). 3.3% of the particles display the cubic morphology framed by cube with slightly lower indices（$0 < \alpha < 1.5$） than that framed by octahedron. The shape mentioned above may be regrown from bars in original seeds or needle-shape particles. Though 5.6% of the particles having the structural characteristics of diamond, cube one or two facets of the crystal might be along with broken problems, which happens randomly and could be attributed to the bombardment of the active particles on the crystal during the growth process. Another 5.6% of the particles with irregular shapes mostly are twined or poly-crystals, obviously due to the seeds aggregation or close distances between the seeds. Besides, there is no too-long bar particles to be found. The crystal shape inspection results show that the powders evidently belong to 2-type superior diamond powders. The inspection results of diamond purity and the grain integrity shown in Figure 1(c) and Figure 2 demonstrate one sharp diamond typical peak at 1,330 cm^{-1} with full width at half maxima (FWHM) valuing around 11–12 cm^{-1} and other locations smooth and without typical graphite or amorphous carbon peaks in all screened particles. The calculated quantitative index of crystal quality q is greater than 99%. EBSD results show the pole graphics of {100}, {110}, and {111}, demonstrating that the particles are characterised with typical cubic crystal, sampling orientation concentrated, and no extra poles, which signifies well growth grains without existence of twins and lattice flaws.

As for M3/6 commercial diamond powders, original seeds are covered by new regrown diamond faces after 120 min boron-doping (500 ppm) deposition, shown in Figure 1(d). 700,000 CVD monocrystalline diamonds are obtained in one deposition over 100 cm^2 substrate. Five hundred randomly picked particles are carried on with size and morphology statistics, shown in Figure 1 and Table 6. The results show with numbers of the particles totalling about 73% of the sample particles, the sizes mainly fall into 4–8 μm, matching the nominal size range and coarse end size requirement of M4/8 powders. However, 23% particles existing in the powders are characterised with the unwanted spontaneous nuclei, and 0.8 μm minimal diameter of fine end D_5, obviously against the corresponding M4/8 standard. The morphology statistics show that 76.5% particles produced with cubic crystal ($1.5 \leq \alpha < 3$) are framed by octahedron. 21.2% particles are with hexahedron-octahedron structure, shape like cube. Compared with the

M0.5/1 fixed powders, the number of the former crystal type particles rises significantly, mainly attributed to that the coarse seed has a strong flaw copy effect. Fortunately, the large size seeds lead to better scattered seeds via the seeding method, thus twined or poly-crystals, i.e., irregular shape particles numbering lower, only accounting 2.3%. The crystal shape results attribute the powders to 2-type high quality crystal shape diamond powder. The quality check for the powders are shown in Figure 1(f) and Figure 3, where 1,332 cm^{-1} typical characteristic diamond peak occurs with FWHM at 12–13 cm^{-1}, and the boron addition leads to a wide peak at 500 cm^{-1} but no obvious effect on the whole purity of diamond since q calculated still over 99%. The EBSD results shown for {100}, {110} and {111} pole graphics demonstrate the crystal orientation concentrated and no extra poles, signifying well growth and no twin or lattice flaw structure located in the particles.

Table 6 The morphology statistic results of CVD microcrystalline diamonds grown on W1 and W5 seeds

Morphological features	*FESEM*	*Ratios*		*Reason*
		W1 (M0/1)	*W5 (M3/6)*	
Hexahedron-octahedron shapes ($1.5 \leq \alpha < 3$)		85.5%	76.5%	Certain environment
Hexahedron-octahedron shapes ($0 < \alpha < 1.5$)		3.3%	21.2%	Bar-shape or needle-shape seeds
Imperfect crystal shape (crystal face broken)		5.6%	0	Random bombardment of active ions
Bicrystal or polycrystalline (irregular shape)		5.6%	2.3%	Seeds aggregation

Figure 1 (a and d) FESEM micrograph, (b and e) grain size distribution, and (c and f) micro-Raman spectra of CVD microcrystalline diamonds grown on W1 and W5 seeds (see online version for colours)

W1(M0/1)

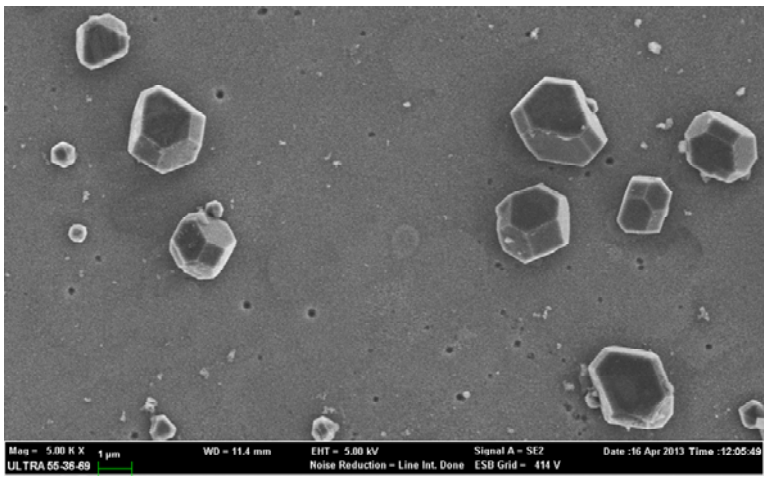

(a)

Figure 1 (a and d) FESEM micrograph, (b and e) grain size distribution, and (c and f) micro-Raman spectra of CVD microcrystalline diamonds grown on W1 and W5 seeds (continued) (see online version for colours)

W1(M0/1)

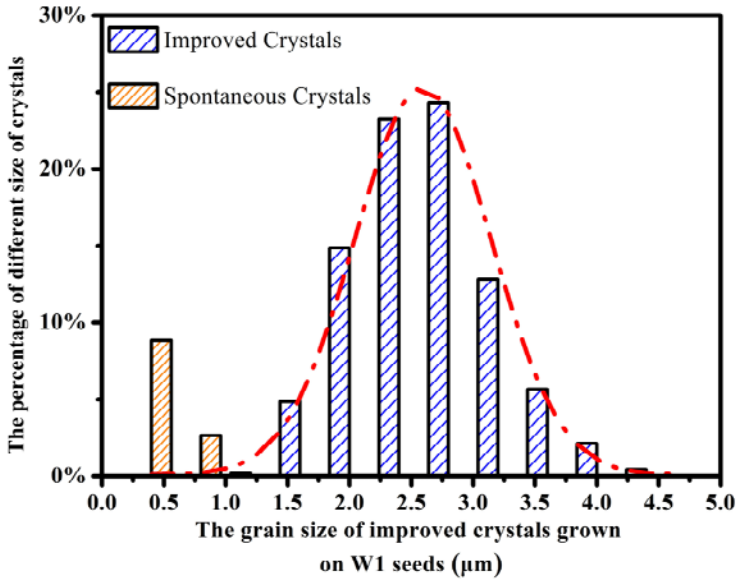

(b)

W1(M0/1)

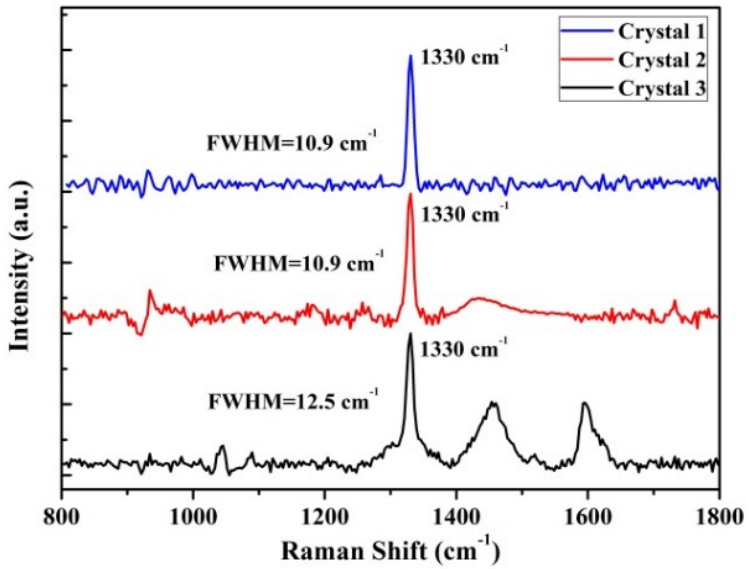

(c)

Figure 1 (a and d) FESEM micrograph, (b and e) grain size distribution, and (c and f) micro-Raman spectra of CVD microcrystalline diamonds grown on W1 and W5 seeds (continued) (see online version for colours)

W1(M0/1)

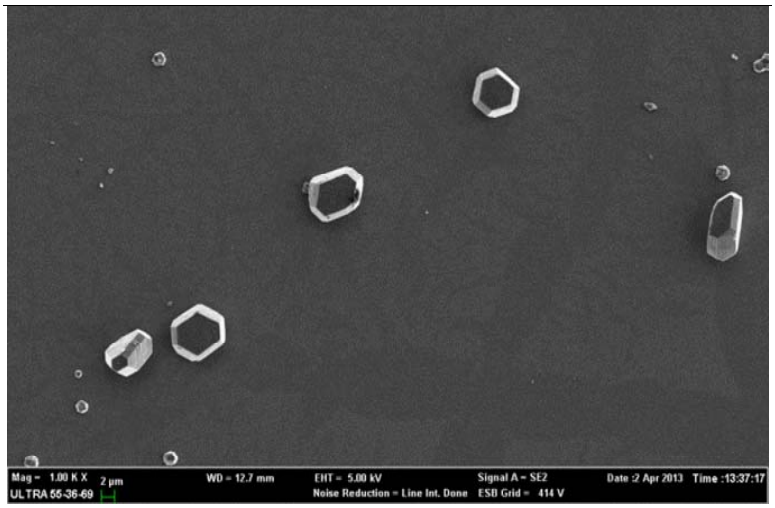

(d)

W5(M3/6)

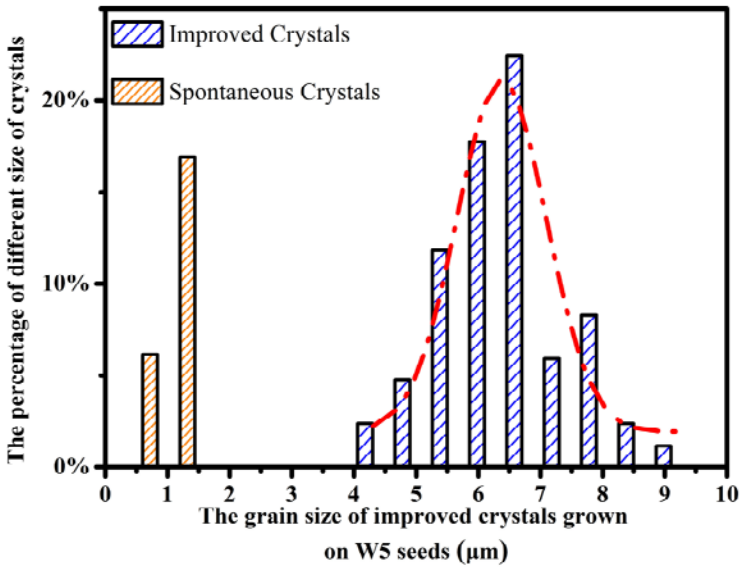

(e)

Figure 1 (a and d) FESEM micrograph, (b and e) grain size distribution, and (c and f) micro-Raman spectra of CVD microcrystalline diamonds grown on W1 and W5 seeds (continued) (see online version for colours)

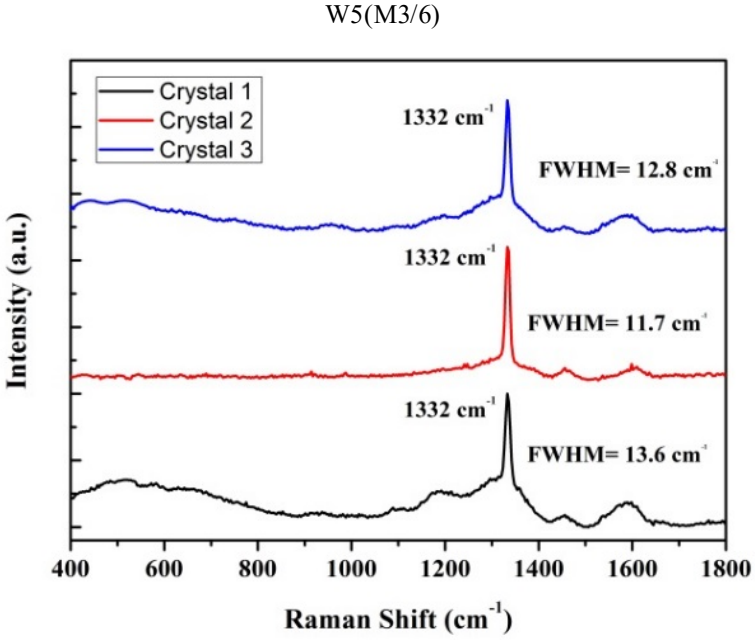

(f)

The test results demonstrate that the diamond single crystal particles made by seeds have absolute advantage over those by traditional crushing method in morphology and surface roughness, whose morphology is usually better than the 2-type commercial diamond powder. However, it is very difficult to meet the demand of the grain size composition due to the occurrences of spontaneous nuclei on the substrate.

4.2 Quality evaluation of CVD diamond powders by self-nucleation method

The size range of single crystal powder of the diamond by self-nucleation method can be adjusted through deposition time. A limiting deposition time of 120 min (40 min nucleation time and 80 min growth time) is taken to evaluate the crystal powder of the diamond by self-nucleation method.

One hundred ninety million single crystal powders of the diamond by self-nucleation method could be collected at 100 cm^2 preprocessed hetero substrate with 120 min deposition, shown in Figure 4(a). The grain size statistics show that mainly the sizes of the particles lie in 1–3 μm. Among them, 75% particles lie in 1.0–2.0 μm, satisfying the grain size index of M1/2 powders including the nominal size range, coarse end diameter, and fine end diameter, etc. Morphological statistics (Table 7) show that 38.5% particles demonstrate the hexahedron-octahedron structure ($1.5 \leq \alpha < 3$) with mainly (111) plane. It is to be noted that 12.2% crystal powders of the samples display a Wulff polyhedron composed of ten (111) planes and five (100) planes and 20.0% with icosahedron shape composed of 20 (111) planes, both rare in human-made diamond. Generally, the Wulff

polyhedron and the dimpled icosahedron demonstrate the lattice flaws, such as the existence of pit at each five axisymmetric center and the occurrence of groove at each edge (Bühler and Prior, 2000). Some researchers believe multiple twin result in the two morphologies, and then such twinned crystals are called the multiply twinned particles (MTP) (May, 1995). The 2-type grains have five-axisymmetric structure with outer shape like circular. Simple calculations give that the Wulff polyhedron is of b value greater than 70%, and similar γ and Φ values close to those of hexahedron-octahedron, while icosahedron is with b value greater than 80%, $\gamma = 138.19°$, and $\Phi = 300°$. Obviously, the items of the latter are better than those of the former such that the latter type is called high quality monocrystalline in some literature (Wei et al., 1993). Besides, there are 20.4% particles in the statistics with the outer shape like the hexahedron-octahedron or icosahedron and significant surface secondary nucleation, and still 8.9% particles form into the irregular shape due to the crystal agglomeration. The inspection result on the crystal shape shows that the amount of irregular particles reaches slightly over 7%, thereby belonging to type 1 diamond powder. The corresponding Raman spectrum displays the typical diamond characteristic peak for the particle specimen, with FWHM lying between 12 cm^{-1} and 15 cm^{-1} and grain shape quality $q \approx 98\%$. The EBSD characteristic results of the specimen shown in Figure 5 tell that most poles concentrate at determinate positions but some pole points with weak intensity, which defines certain orientation relationship between the 2-type poles, and signifying the twin crystal or lattice flaws structure located in the particles.

Figure 2 The {100}, {110}, and {111} pole figures of CVD microcrystalline diamonds grown on W1 seeds (see online version for colours)

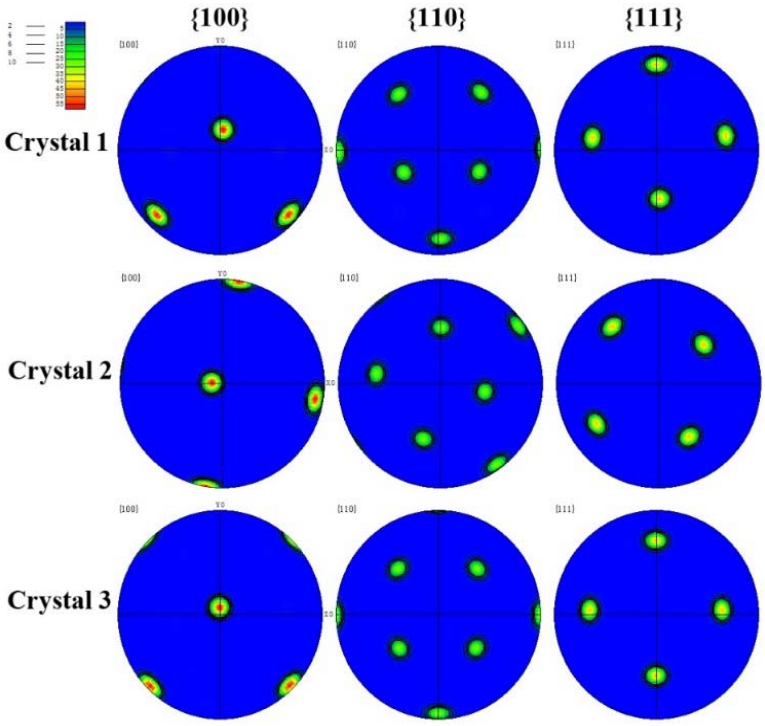

Figure 3 The {100}, {110}, and {111} pole figures of CVD microcrystalline diamonds grown on W5 seeds (see online version for colours)

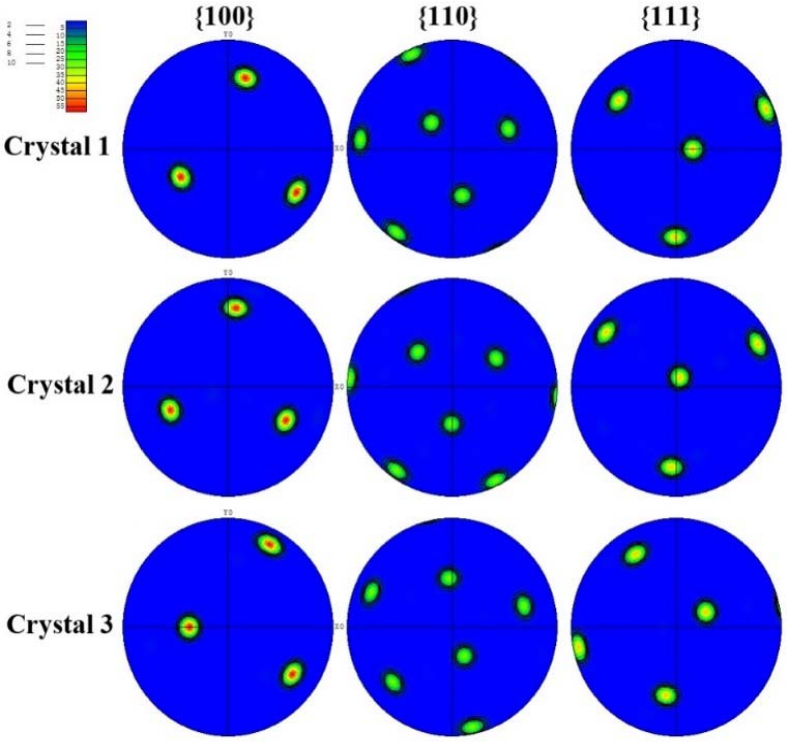

Figure 4 The (a) FESEM micrograph, (b) grain size distribution, and (c) micro-Raman spectra of CVD microcrystalline diamonds grown by the self-nucleation method (see online version for colours)

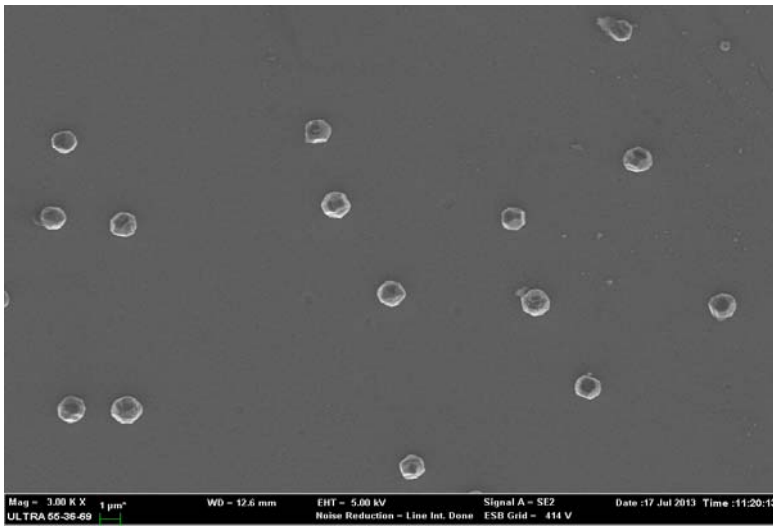

(a)

Figure 4 The (a) FESEM micrograph, (b) grain size distribution, and (c) micro-Raman spectra of CVD microcrystalline diamonds grown by the self-nucleation method (continued) (see online version for colours)

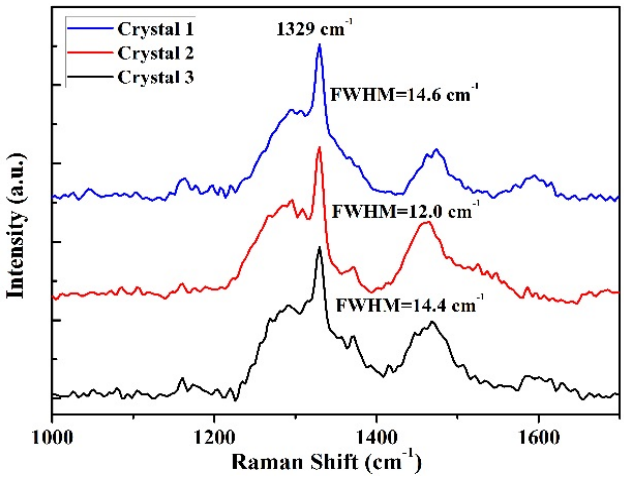

(c)

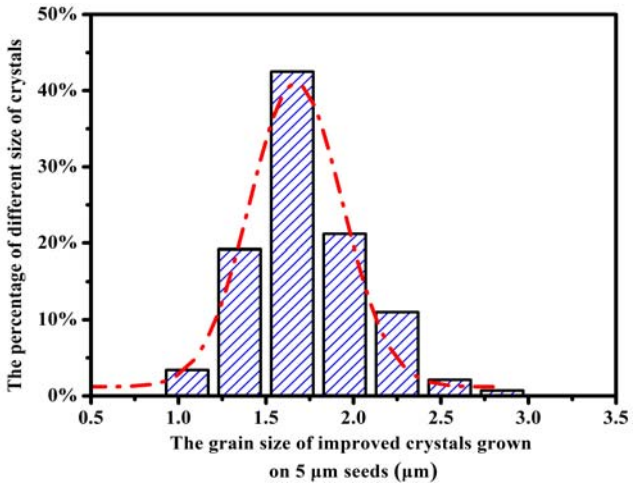

(b)

Compared with diamond crystal powders by seeds, the powders by the self-nucleation method are characterised with more lattice dislocation, distortion, surface secondary nucleation flaws, certain grain aggregation (irregular shape) problems, noticeable trans-polyacetylene peak (1,430–1,470 cm^{-1}), and amorphous carbon peak (1,580 cm^{-1}), which mainly are attributed to the deposition mechanism of the diamond grown by the self-nucleation method (Zhang et al., 2015). Nonetheless, the similarity of initial growth states of the particles processed in the self-nucleation method and the uniform deposition environment generate the well grouped distribution range of the grain size without additional size filtering job.

Table 7 The morphology statistic results of CVD microcrystalline diamonds deposited by self-nucleation method

Morphological features	*FESEM*	*Ratio*	*Reason*
Hexahedron-octahedron polycrystalline ($1.5 \leq \alpha < 3$)		38.5%	Certain environment
Wulff polyhedron		12.2%	Multiple twins
Dimpled icosahedron		20.0%	Multiple twins
Hexahedron-octahedron or icosahedron with surface flaw		20.4%	Surface secondary nucleation
Twin crystal or polycrystal (irregular shape)		8.9%	Non-uniform substrate flaw distribution

Figure 5 The {100}, {110} and {111} pole figure of CVD microcrystalline diamonds grown under the preferred deposition conditions by the self-nucleation method (see online version for colours)

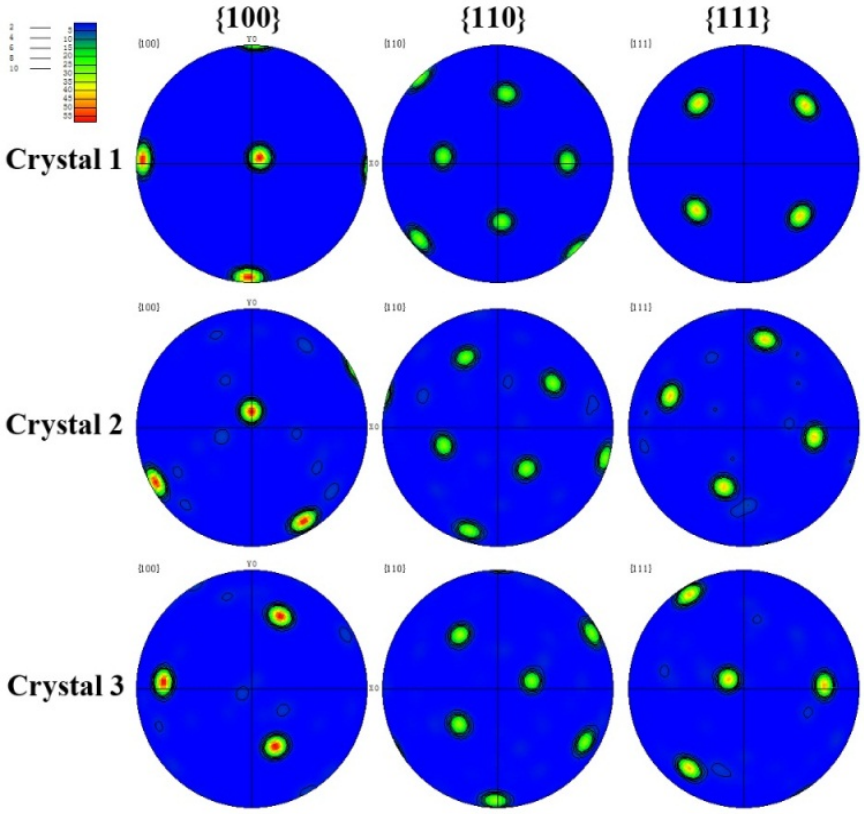

5 Conclusions

CVD diamond powders are fabricated by seeding and self-nucleation method via HFCVD apparatus. With the seeding method, the CVD diamond powders with the average grain size of 2~13 μm can be obtained from the different-sizes seeds by the no-doping or lightly boron-doping technology. With the self-nucleation method, the CVD diamond powders with the average grain size of 0.3~2 μm can be obtained by the lightly boron-doping technology. Then we focus on evaluation of such particles against China industry standard of diamond powders (JB/T 7990-2012). For the particles grown on the seeds, over 80% crystals exhibit a cubo-octahedral with smooth surfaces and no obvious growth defects, and irregular crystals including twined or poly-crystals account for only 2.3%~5.6% of examined ones. The detection results on the diamond purity show that the quantitative index q is greater than 99%. However, the powders cannot meet the corresponding requirements of fine end granularity index (D_5) and median diameter index (D_{50}) due to the existence of 10%–23% spontaneous particles (0.5~1.2 μm). For those powders deposited by self-nucleation method, the test results show that the particle size composition agrees well with the model defined by the industry standard owing to the similarity of initial growth states of the particles. 70.5% crystals exhibit the cubo-octahedral or icosahedron morphology. 20.4% particles have the surface imperfections caused by the unwanted secondary nucleation, and still 8.9% particles form into the irregular shapes due to the crystal agglomeration. Compared with conventional diamond powders obtained from crushing the large-size HPHT diamond, two types of CVD diamond powders have great advantages on the morphology and surface quality. Such well-faceted powders will be more suitable for machining high precision products.

Acknowledgements

This research is supported by the National Natural Science Foundation of China (no. 51605280, 51505192) and Scientific and Technological Innovation Team Foundation (no. 30593118001) and Starting Foundation (no. 30593118006) of Wuxi Institute of Technology.

References

Abreu, C.S., Amaral, M., Oliveira, F.J., Fernandes, A.J.S., Gomes, J.R. and Silva, R.F. (2006) 'Enhanced performance of HFCVD nanocrystalline diamond self-mated tribosystems by plasma pretreatments on silicon nitride substrates', *Diam. Relat. Mat.*, Vol. 15, Nos. 11–12, pp.2024–2028.

Achard, J., Silva, F., Issaoui, R., Brinza, O., Tallaire, A., Schneider, H., Isoird, K., Ding, H., Kon, S., Pinault, M.A. et al. (2011) 'Thick boron doped diamond single crystals for high power electronics', *Diam. Relat. Mat.*, Vol. 20, No. 2, pp.145–152.

Boussadi, A., Tallaire, A., Brinza, O., Pinault-Thaury, M.A. and Achard, J. (2017) 'Thick heavily boron doped CVD diamond films homoepitaxially grown on (111)-oriented substrates', *Diam. Relat. Mat.*, Vol. 79, No. 9, pp.108–111.

Bühler, J. and Prior, Y. (2000) 'Study of morphological behavior of single diamond crystals', *J. Cryst. Growth*, Vol. 209, No. 4, pp.779–788.

Chakraborty, R. and Sharma, S.C. (2011) 'Structure of diamond nanoparticles grown by chemical vapor deposition', *Physica B*, Vol. 406, No. 22, pp.4170–4174.

Chung, H-K. and Sung, J.C. (2001) 'The CVD growth of micro crystals of diamond', *Diam. Relat. Mat.*, Vol. 10, Nos. 9–10, pp.1584–1587.

Filatov, Y.D., Vetrov, A.G., Sidorko, V.I., Filatov, A.Y. and Kovalev, S.V. (2013) 'A mechanism of diamond-abrasive finishing of monocrystalline silicon carbide', *J. Superhard Mater.*, Vol. 35, No. 5, pp.303–308.

Gicquel, A., Hassouni, K., Silva, F. and Achard, J. (2001) 'CVD diamond films: from growth to applications', *Current Applied Physics*, Vol. 1, No. 6, pp.479–496.

Hirmke, J., Schwarz, S., Rottmair, C., Rosiwal, S.M. and Singer, R.F. (2006) 'Diamond single crystal growth in hot filament CVD', *Diam. Relat. Mat.*, Vol. 15, Nos. 4–8, pp.536–541.

Iniesta, J., Michaud, P.A., Panizza, M., Cerisola, G., Aldaz, A. and Comninellis, C. (2001) 'Electrochemical oxidation of phenol at boron-doped diamond electrode', *Electrochim. Acta*, Vol. 46, No. 23, pp.3573–3578.

Konoplyuk, S., Abe, T., Takagi, T. and Uchimoto, T. (2007) 'Hot filament CVD diamond coating of TiC sliders', *Diam. Relat. Mat.*, Vol. 16, No. 3, pp.609–615.

Linares, R. and Doering, P. (1999) 'Properties of large single crystal diamond', *Diam. Relat. Mat.*, Vol. 8, Nos. 2–5, pp.909–915.

May, P.W. (1995) 'CVD diamond: a new technology for the future?', *Endeavour*, Vol. 19, No. 3, pp.101–106.

Schreck, M., Grunick, C., Haug, C., Brenn, R. and Stritzker, B. (2002) 'Bias assisted growth on diamond single crystals: the defect formation due to ion bombardment studied by ion channelling, electron backscatter diffraction, and micro-Raman spectroscopy', *Diam. Relat. Mat.*, Vol. 11, Nos. 3–6, pp.487–492.

Schwarz, S., Rottmair, C., Hirmke, J., Rosiwal, S. and Singer, R.F. (2004) 'CVD-diamond single-crystal growth', *J. Cryst. Growth*, Vol. 271, Nos. 3–4, pp.425–434.

Shu, G., Dai, B., Ralchenko, V.G., Bolshakov, A.P., Khomich, A.A., Ashkinazi, E.E., Yurov, V.Y., Yao, K., Liu, K., Zhao, J. et al. (2018) 'Vertical-substrate epitaxial growth of single-crystal diamond by microwave plasma-assisted chemical vapor deposition', *J. Cryst. Growth*, Vol. 486, No. 6, pp.104–110.

Silva, F., Gicquel, A., Tardieu, A., Cledat, P. and Chauveau, T. (1996) 'Control of an MPACVD reactor for polycrystalline textured diamond films synthesis: role of microwave power density', *Diam. Relat. Mat.*, Vol. 5, Nos. 3–5, pp.338–344.

Sochr, J., Švorc, Ľ., Rievaj, M. and Bustin, D. (2014) 'Electrochemical determination of adrenaline in human urine using a boron-doped diamond film electrode', *Diam. Relat. Mat.*, Vol. 43, No. 3, pp.5–11.

Stacey, A., Aharonovich, I., Prawer, S. and Butler, J.E. (2009) 'Controlled synthesis of high quality micro/nano-diamonds by microwave plasma chemical vapor deposition', *Diam. Relat. Mat.*, Vol. 18, No. 1, pp.51–55.

Sun, F., Ma, Y., Shen, B., Zhang, Z. and Chen, M. (2009) 'Fabrication and application of nano-microcrystalline composite diamond films on the interior hole surfaces of Co cemented tungsten carbide substrates', *Diam. Relat. Mat.*, Vol. 18, Nos. 2–3, pp.276–282.

Sung, C.M. (1999) 'Brazed diamond grid: a revolutionary design for diamond saws', *Diam. Relat. Mat.*, Vol. 8, Nos. 8–9, pp.1540–1543.

Wada, N. and Solin, S.A. (1981) 'Raman efficiency measurements of graphite', *Physica B+C*, Vol. 105, No. 1, pp.353–356.

Wei, Z., Kong, H.S. and Glass, J.T. (1993) *Diamond Films and Coatings*, pp.293–295, Noyes Pub., Park Ridge.

Yan, C.S., Mao, H.K., Li, W., Qian, J., Zhao, Y. and Hemley, R.J. (2004) 'Ultrahard diamond single crystals from chemical vapor deposition', *Phys. Stat. Sol.*, Vol. 201, No. 4, pp.R25–R27.

Zhang, T. and Zou, Y. (2017) 'The effect of deposition parameters on the growth rate of microcrystalline diamond powders synthesized by HFCVD method', *Coatings*, Vol. 7, No. 7, p.95.

Zhang, T., Liu, X., Sun, F. and Zhang, Z. (2015) 'The deposition parameters in the synthesis of CVD microcrystalline diamond powders optimized by the orthogonal experiment', *J. Cryst. Growth*, Vol. 426, No. 18, pp.15–24.

Zhang, T., Wang, X.C., Shen, B., Sun, F.H. and Zhang, Z.M. (2013a) 'The effect of deposition parameters on the morphology of micron diamond powders synthesized by HFCVD method', *J. Cryst. Growth*, Vol. 372, No. 11, pp.49–56.

Zhang, T., Wang, L., Sun, F., Shen, B. and Zhang, Z. (2013b) 'The effect of boron doping on the morphology and growth rate of micron diamond powders synthesized by HFCVD method', *Diam. Relat. Mat.*, Vol. 40, No. 10, pp.82–88.